EXPERIMENTAL RESEARCH ON DYNAMIC PERFORMANCE OF AN AIR/WATER SOURCE HEAT PUMP WATER HEATER

by

Fuqiang QIU[a,e*], Juanli DU[b], Yu WANG[a], Xingwei ZHANG[c], Changsuo YU[d], and Yun NAN[d]

[a] School of Electrical Engineering, Tongling University, Tongling, China
[b] School of Energy and Intelligent Engineering,
Henan University of Animal Husbandry and Economy, Zhengzhou, China
[c] Xinxiang Chemical Fiber Co., Ltd, Xinxiang, China
[d] Tongling Polytechnic, Tongling, China
[e] Hong'an Solar Energy Co., Ltd, Tongling, China

Original scientific paper
https://doi.org/10.2298/TSCI2403067Q

In this paper, a combined air/water source heat pump water heater is presented. At ordinary time, the heater can be used for hot water heating in water-source mode to improve the energy efficiency. While in cold season, it gives priority to air-source mode for water heating to improve operational safety. Experiments were conducted to investigate the thermodynamic performance of the heater in each operation mode, and the experiment results were analyzed. The research indicated that its operation was reliable during the long-time running. This paper offers a promising energy-saving method in future.

Key words: *hydrology, dual source, heat pump water heater, energy saving, new technology of refrigeration, COP*

Introduction

The energy crisis [1, 2] and environmental pollution [3, 4] have become the major problems facing mankind in the world. The energy consumption of supplying hot water for building accounts for 23.4% of the total building energy consumption [5], and the concepts of the passive solar buildings [6], and energy harvesting systems [7] were appeared in literature for green energy.

Heat pump (HP) [8] for renewable energy technology, including ground source (GSHP) [9], air source (ASHP) [10], and water source (WSHP) [11], has been rapidly developed in recent years due to its relatively high energy efficiency and environmental friendliness [12, 13]. Thus, the potential of economic and environmental benefits in residential water bath is enormous. However, it also encountered a development bottleneck in the further improvement of energy efficiency. It is a hot research direction in the future to further improve the year-round operation energy efficiency of heat pump water heaters, and thermal science [14] will play an important role in making it more energy-saving.

In recent years, various dual source heat pump water heaters have been presented to further improve energy efficiency. For examples, Lazzarin [15] presented two kinds of dual

* Corresponding author, e-mail: 549977856@qq.com

source heat pumps systems, Xu *et al.* [16] and Deng and Yu [17] studied a solar-air source heat pump water heater, Aguilar *et al*. [18] proposed a PV assisted compact heat pump water heater, Cai *et al*. [19] presented a new type of PV/T-air dual source heat pump water heater, Cai *et al*. [20] proposed a solar-air dual series source heat pump water heater. Zhao *et al*. [21] performed an energetic, economic and environmental evaluation on an air-flue gas dual-source heat pump. The mentioned dual source heat pump water heaters have significant energy efficiency.

Water-source heat pump water heat system [22] has higher COP than that of air source heat pump. However, it cannot operate safely in cold weather due to frost. This paper presented a combined air/water source heat pump (AWHP) water heater for a bathroom unit, it can produce hot water in water-source mode at ordinary times to improve energy efficiency, and produce hot water in air-source mode in cold weather to ensure safe operation. Experiments were conducted to analyze the thermostatic performance of the heater in each mode.

Experimental set-up

In the AWHP, an air-source evaporator and a water-source evaporator are arranged, a reversing valve (RV) and three solenoid valves (SV) are used to control whether air-source or water-source mode is used to produce hot water. The basic principle of the heater is shown in fig. 1, and the photo of the experimental equipment is shown in fig. 2. The detailed specifications of the heater are listed in tab. 1.

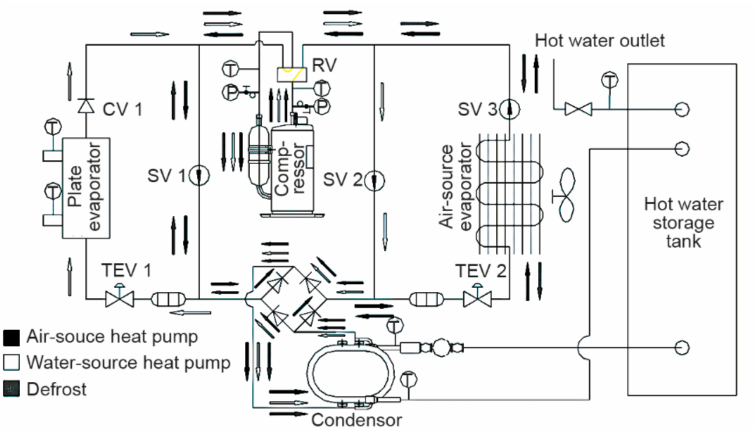

Figure 1. Sketch of the combined AWHP

In water-source mode at ordinary times, SV1 and SV3 are turned off, SV2 is open on, and RV is on, the refrigerant flow direction is indicated by hollow arrows.

In air source mode in cold season, SV1 and SV3 are opened, SV2 is off, the refrigerant flow direction is indicated by solid arrows.

In defrosting mode, the refrigerant flow direction is shown by half hollow arrows. the RV is shift, SV1 and SV3 are on, and SV2 is off.

In the experiment, an enthalpy laboratory (GB/T17758-2010) located in Nantong, China was used to simulate the testing ambient. The testing environments are presented in tab. 2, and the experimental measurements are listed in tab. 3. Individual air-handling unit (AHU) was utilized to control the air temperature and relative humidity of the chamber. An electric heater is used to simulate the inlet water temperature at the evaporation side in water-source mode, and the hot water flowing rate is 5.2 m^3/h.

In this paper, the COP of the AWHP was defined

$$\mathrm{COP} = \frac{Q}{W} = \frac{\rho c V (t_{w2} - t_{w1})}{\Delta t \Delta P} \tag{1}$$

where Q [kW] is the output capacity, W [kW] – the input power, ρ – the water density (ρ = 1000 kg/m^3), c_p – the specific heat of water at constant pressure (c_p = 4.186 kJ/kgK), V – the volume of the water tank (V = 0.15 m^3), t_{w1} and t_{w2} [°C] – the initial and final water temperatures in the tank, respectively, Δt [hour] – the time interval, W [kW] – the input power, and ΔP [Pa] – pressure gradient.

Figure 2. Photo of the experimental equipment

Table 1. Specifications of the main components of the system

AWHP water heater	Quantity	Specification
Nominal water heating capacity		25 kW
Compressor	2	Sanyo: C-SB453H8A
Working fluid		R22
Air-source evaporator and condenser	1	Hydrophilic film corrugated aluminum fins (ptlon: 25.1 mm, pttra: 25.1 mm, δ: 0.13 mm) Inner grooved copper tubes (OD: 9.52 mm, δ: 0.5 mm)
Plate heat exchanger	64	EATB55
Thermostatic expansion valve	1	BAE 7
Double-pipe heat exchanger	1	Tailored
Inner tube	3	External thread copper (ID: 16.3 mm, OD: 19 mm, length: 4680 mm)
Outer tube	3	Seamless steel tube (ID: 25 mm, OD: 28 mm, length: 4630 mm)
Insulation layer		Black waterproof rubber thermal board
Water tank	1	530 L
Liner		Stainless steel
Insulation layer		Polystyrene foamed plastic

OD: out diameter, ID: inner diameter

Table 2. Testing environment of the AWHPW

Testing conditions	Ambient temperature in outdoor chamber [°C]		Inlet water temperature at evaporator side [°C]		Mean water temperature in water tank [°C]	
Air-source	Dry bulb	Wet bulb	t_{w1}	t_{w2}	t_{w1}	t_{w2}
	20	15			15	55
Water-source	2	1				
			15		–20 °C	60 °C

Table 3. Summary of the measuring instruments

Parameters	Instrument	Model	Range	Accuracy
Air temperature and humidity	Thermometer	Rotronic HygroFlex	–40 ~ 85 °C	±0.1 °C ±1% RH
Supply air flow rate	Thermal anemometer	E+E 70-VT62B5	0 ~ 5 m/s	±2% F.S
Water temperature	Pt100 RTD	Omega 1/10 DIN	–100 ~ 400 °C	±0.05 °C
Refrigerant temperature	Thermocouple	K-type	0 ~ 1250 °C	±0.1 °C
Refrigerant pressure	Pressure gauge	Bourdon	–0.1 ~ 1.2 MPa –0.1 ~ 3.4 MPa	±0.3% F.S.
Power consumption	Power meter	FLUKE 39	0 ~ 10 kW	±2%

Results and discussion

Figure 3(a) shows the variations of the refrigeration pressure and pressure ratio of the AWHP in air-source mode. The discharge pressure revealed a continuous upward trend versus hot water temperature due to the reduction of the heat transfer temperature difference between refrigerant and hot water. While the suction pressure is basically unchanged due to the auto-regulation of the thermostatic expansion valve. An increase in the pressure ratio will reduce the mass flux of refrigerant flowing through the compressor.

The suction pressure of the AWHP at 20 °C condition is significantly higher than that at 7 °C condition, which is due to the increased vaporization of refrigerant in the evaporator. At this time, in order to maintain a constant degree of superheat, the opening of the expansion valve increases, causing an increase in the amount of refrigerant flowing into the evaporator. It also causes an insignificant increase in discharge pressure.

Figure 3(b) shows the changes of refrigerant temperature of the AWHP in air-source mode under the conditions of 20 °C and 7 °C. As the temperature of hot water increases, the discharge temperature also presents a continuous upward trend. This is due to an increase in the pressure ratio causing a decrease in the mass flux of refrigerant flowing through the compressor, resulting in a deterioration in the cooling effect of the refrigerant on the compressor.

The suction temperature on conditions of 7 °C ambient temperature is lower than that on conditions of 20 °C due to the decrease of refrigerant evaporation temperature in the evaporator. Due to the increase of compression ratio, the discharge temperature of the system is higher than that on conditions of 20 °C ambient temperature.

It can be seen from fig. 3(c) that the transient water heating power, Q_{wh}, of the AWHP in air-source mode exhibits a decreasing process with the hot water temperature, which is attributed to a decrease in the mass flux of the refrigerant flowing through the compressor caused by a decrease in the pressure ratio. The heating power at 20 ℃ is significantly higher than that at 7 ℃. The Q_{wh} at 20 ℃ is significantly higher than that at 7 ℃.

It can also be observed from fig. 3(c) that the instantaneous input power, W, undergoes a continuously increasing process due to the increase in input work per unit mass of refrigerant. In addition, since the mass-flow rate of the refrigerant flowing through the compressor at 20 ℃ is greater than that at 7 ℃, the W at 20 ℃ is higher than that at 7 ℃. The average Q_{wh} at 20 ℃ and 7 ℃ are 6.35 and 6.09 kW, respectively.

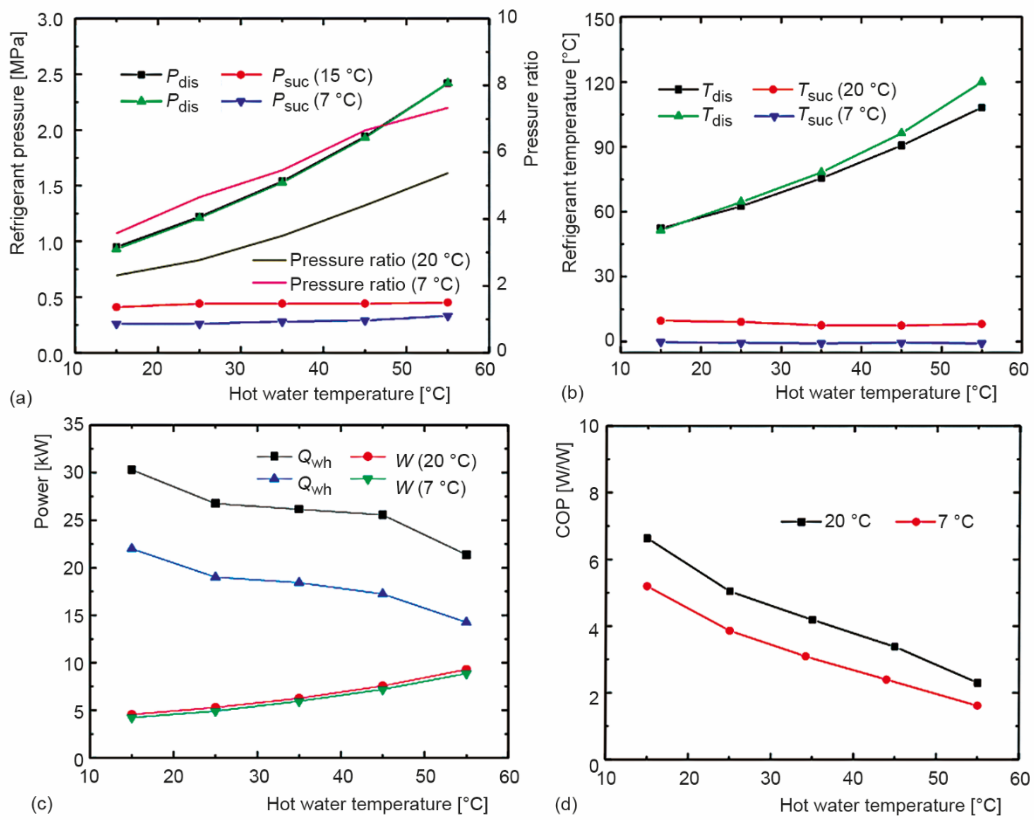

Figure 3. Variations of (a) suction and discharge pressure, (b) suction and discharge temperature, (c) power, and (d) COP of the AWHP in air-source mode

As observed from fig. 3(d) that the instantaneous COP of the AWHP drops with hot water temperature due to the decline of Q_{wh} and the ascend of W, and the gap between the two gradually narrows. The COP of the AWHP under 20 ℃ condition is 4.16, which is significantly higher than that of 3.24 under 7 ℃ condition.

The performance of the AWHP is studied at 15 ℃ inlet water temperature at the evaporation side. The specific results are shown in fig. 4. In order to avoid repetition, the reason for curve variation are detailed in this part.

It can be seen from fig. 4(a) that the discharge pressure of the AWHP increases rapidly with the upswing of hot water temperature. However, the suction pressure is slightly increased due to the auto-regulation of the thermal expansion valve.

Figure 4(b) shows the changes of suction and discharge temperature of the AWHP in water-source mode. It can be seen from fig. 4(b) that with the upswing of the hot water temperature, the exhaust temperature of the system is gradually rising and the rising speed is gradually accelerating due to the insufficient cooling of the compressor caused by the decrease of the refrigerant flow through the compressor. Due to the self-regulation of the thermal expansion valve, the suction temperature of the CAWHP is basically kept at a constant value. However, the refrigerant flow rate entering the evaporator is not absolutely stable, so its value changes slightly.

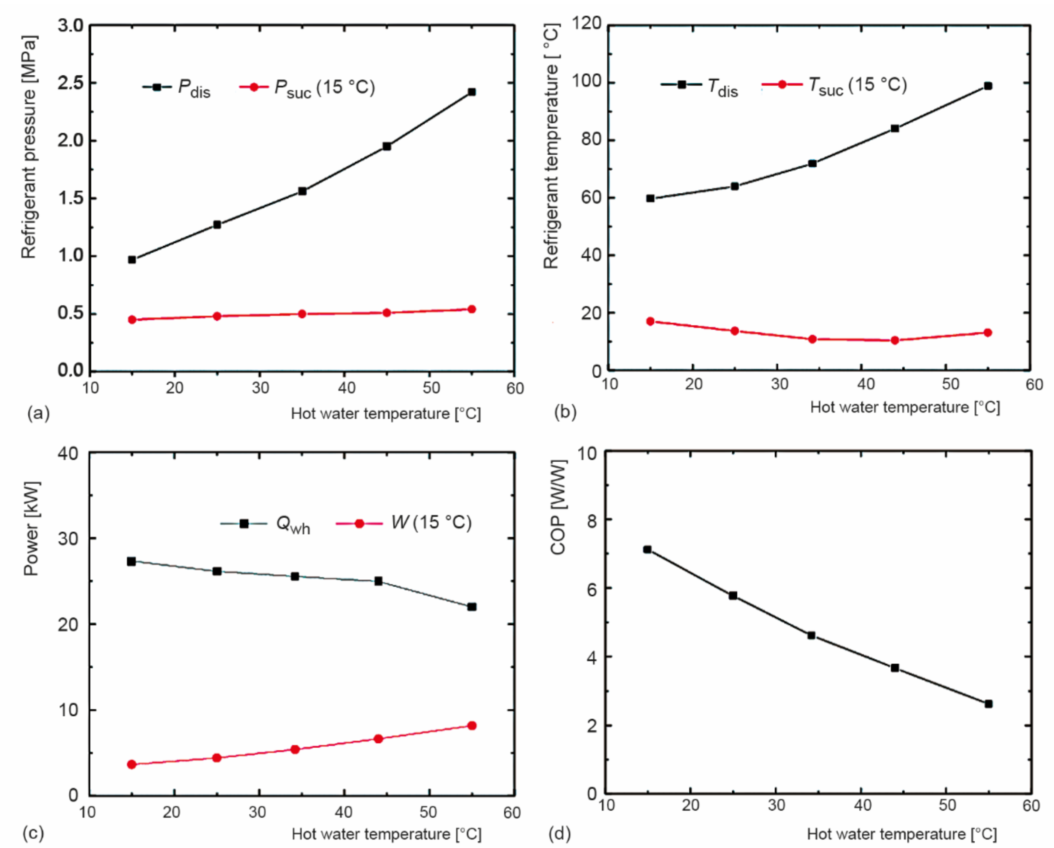

Figure 4. Variations of (a) suction and discharge pressure, (b) suction and discharge temperature, (c) power, and (d) COP of the AWHP in air-source mode

Figure 4(c) shows the variations in power of the AWHP with hot water temperature in water-source mode. As seen from fig. 4, with the rising of the hot water temperature, the water heating power of the AWHP is gradually reduced due to the decrease of the mass-flow rate of refrigerant flowing through the compressor into the condenser. The instantaneous input power of the AWHP is gradually increasing, and its rising trend is also increasing due to the increase of input power of unit mass refrigerant, although the mass-flow rate of refrigerant flowing through the compressor is reduced at this time.

Figure 4(d) shows the variation of COP with hot water temperature in water-source mode. It can be seen from fig. 4(d) that the COP of the AWHP is gradually decreasing with the upswing of the hot water temperature. The results show that the total COP of the AWHP is 4.65.

Conclusions

In order to further improve the efficiency of heat pump water heater, the AWHP was proposed and designed, and its operation mechanism was fully unlocked experimentally, especially the effects of pressure, temperature and power on COP were revealed in air source and water source mode. Some conclusions are summarized as follows.

- In ordinary time, the water-source mode is used to produce hot water, the heating power is 25.95 kW and the COP_{wh} is 4.65 when the inlet water temperature is 15 °C.
- In cold season, the air-source mode is used to produce hot water, the heating power of the system is 26.42 kW and the COP_{wh} is 4.16 when the ambient temperature is 20 °C; the heating power is 9.72 kW and the COP_{wh} is 3.24 when the ambient temperature is 7 °C.

Acknowledgment

This work was financially supported by the Talent scientific research start-up fund project of Tongling University (2021tlxyrc25), and the Natural Science Research Project of Tongling University: Research on system identification and Operation Optimization of Thermal electric Integrated Energy (2022tlxy46).

References

[1] Goldthau, A., Tagliapietra, S., Energy Crisis: Five Questions that Must be Answered in 2023, *Nature, 612* (2022), Dec., pp. 627-630
[2] Crew, B., Solving the Energy Crisis, *Nature, 609* (2022), Sept., pp. S1-S1
[3] Perera, F. P., *et al*., Molecular and Genetic-Damage in Humans from Environmental Pollution in Poland, *Nature, 360* (1992), Nov., pp. 256-258
[4] Mitrovic, D., *et al*., Energy Analysis of Repowering Steam Power Plants by Feed Water Heating, *Facta Universitatis Series: Mechanical Engineering, 20* (2022), 1, pp. 53-72
[5] Nam, Y., *et al*., Development of Dual-Source Hybrid Heat Pump System Using Groundwater and Air, *Energy Build, 42* (2010), 6, pp. 909-916
[6] Ma, J., *et al*., Optimal Design of Passive Solar Building, *Thermal Science, 26* (2022), 3, pp. 2453-2458
[7] He, C. H., *et al*., Controlling the Kinematics of a Spring-Pendulum System Using an Energy Harvesting Device, *Journal of Low Frequency Noise, Vibration & Active Control, 41* (2022), 3, pp. 1234-1257
[8] Huang, D. S., *et al*., Evaluation of Thermal Performance of Air Source Heat Pump Heating System Based on Electricity Equivalent, *Thermal Science*, *26* (2022), 5B, pp. 4207-4216
[9] Ikeda, S., *et al*., Optimization Method for Multiple Heat Source Operation Including Ground Source Heat Pump Considering Dynamic Variation in Ground Temperature, *Appl. Energy, 193* (2017), May, pp. 466-478
[10] Xu, Y., *et al*., Experimental Investigation on an Ultra-High Temperature Air Source Heat Pump Water Heater, *J. Thermal Sci. Eng. Appl, 13* (2021), 6, pp. 1-20
[11] Fan, F., *et al*., The Influence of Internal Heat Exchanger on the Performance of Transcritical CO_2 Water Source Heat Pump Water Heater, *Energies, 13* (2020), 7, 1787
[12] Sonawan, H., Hakkiki, J., Performances and Economics of Heat Pump Water Heater, *International Journal of Energy for a Clean Environment, 22* (2021), 5, pp. 51-64
[13] Biao, X., *et al*., Annual Performance Analysis of an Air Source Heat Pump Water Heater Using a New Eco-Friendly Refrigerant Mixture as an Alternative to R134a, *Renewable Energy, 147* (2020), 1, pp. 2013-2023

[14] Qian, M. Y., He, J.-H., Two-Scale Thermal Science for Modern Life: Making the Impossible Possible, *Thermal Science*, *26* (2022), 3B, pp. 2409-2412
[15] Lazzarin, R. M., Dual Source Heat Pump Systems: Operation and Performance, *Energy and Buildings*, *52* (2012), Sept., pp. 77-85
[16] Xu, G., *et al*., A Simulation Study on the Operating Performance of a Solar-Air Source Heat Pump Water Heater, *Applied Thermal Engineering*, *26* (2006), 11-12, pp. 1257-1265
[17] Deng, W. S., Yu, J. L., Simulation Analysis on Dynamic Performance of a Combined Solar/Air Dual Source Heat Pump Water Heater, *Energy Conversion and Management*, *120* (2016), July, pp. 378-387
[18] Aguilar, F., *et al*., Environmental Benefits and Economic Feasibility of a Photovoltaic Assisted Heat Pump Water Heater, *Solar Energy*, *193* (2019), Nov., pp. 20-30
[19] Cai, J. Y., *et al*., A Novel PV/T-Air Dual Source Heat Pump Water Heater System: Dynamic Simulation and Performance Characterization, *Energy Conversion and Management*, *148* (2017), Sept., pp. 635-645
[20] Cai, J. Y., *et al*., Analysis and Optimization on the Performance of a Heat Pump Water Heater with Solar-Air Dual Series Source, *Case Studies in Thermal Engineering*, *28* (2021), 101577
[21] Zhao, R., *et al*., An Energetic, Economic and Environmental Evaluation of a Dual-Source Heat Pump Water Heater – A Case Study in Beijing, *Energy Conversion and Management, 253* (2022), 115190
[22] Zhao, Z. C., *et al*., Experimental Research of a Water-Source Heat Pump Water Heater System, *Energies*, *11* (2018), 5, 1205

Paper submitted: November 1, 2022
Paper revised: April 10, 2023
Paper accepted: May 21, 2023